Effect of random positions for coherent dipole transport

F. Robicheaux[1,*] and N. M. Gill[2]
[1]*Department of Physics, Purdue University, West Lafayette, Indiana 47907, USA*
[2]*Department of Physics, Auburn University, Auburn, Alabama 36849, USA*
(Received 19 January 2014; published 30 May 2014)

We calculate the effect of two kinds of randomness on the coherent motion of an exciton whose transport is governed by the dipole-dipole interaction. As our example, we use the idealized case of stationary Rydberg atoms on a lattice. We present calculations for how fast the excitation can move away from its starting position for different dimensional lattices and for different levels of randomness. We also examine the asymptotic in time final position of the excitation to determine whether or not the excitation can be localized. The one-dimensional system is an example of Anderson localization where the randomness is in the off-diagonal elements although the long-range nature of the interaction leads to nonexponential decay with distance. The two-dimensional square lattice shows a mixture of extended and localized states for large randomness, while there is no visible sign of localized states for weak randomness. The three-dimensional cubic lattice has few localized states even for strong randomness.

DOI: 10.1103/PhysRevA.89.053429 PACS number(s): 32.80.Ee, 34.20.Cf, 37.10.Jk

I. INTRODUCTION

The interaction of many atoms and/or molecules can lead to a rich variety of processes. There has been recent interest in the physics of many atoms interacting with each other through the dipole-dipole potential. This interest is spurred by the developments in experiments and calculations of cold gases. There have been studies of amorphous systems where the atoms (molecules) have a random placement as well as theoretical studies of atoms (molecules) placed on perfect lattices. The purpose of this paper is to present results of a system with the atoms placed in a lattice but with some randomness in the placement. In particular, we investigate how the randomness affects the motion of an exciton whose coherent motion is only determined by the dipole-dipole interaction while the atoms remain fixed.

The system discussed in this paper is a lattice of idealized Rydberg atoms with dipole-dipole interactions. This system is a more regular arrangement of atoms but is otherwise similar in spirit to the original experiments on Rydberg gases [1,2]. In these experiments, a dense Rydberg gas was achieved by exciting many atoms to a Rydberg state and the subsequent dipole-dipole interactions between atoms caused the state to change; the new states could then coherently move through the sea of unchanged states. We will treat an idealized case of a lattice of Rydberg atoms where every atom except one is in a highly excited s state and the exception is a p state. Because of the dipole-dipole interaction, the p state can coherently move from atom to atom. Our simplifications are to ignore terms higher than dipole-dipole in the interaction, to fix the atoms in space, and to ignore radiative decay.

The dipole-dipole interaction can lead to a wide variety of effects which have implications for exciton transport. For examples of this situation, we will look to recent results on Rydberg gases, since we will treat an ideal case of this system. Possibly the most important effect arises because the diagonal term in the Hamiltonian is the same for all states, while the off-diagonal term depends on the separation. Since the interaction strongly depends on separation, two atoms that are somewhat closer together than average will appear to be two states with shifted energies. Reference [3] described calculations that showed the strongly interacting Rydberg atoms could shift the energy of the pair out of resonance, which provides a blockade to further excitation. Reference [4] provided experimental evidence for this effect by showing the number of Rydberg atoms excited in a dense gas did not scale linearly with the laser power. Extreme examples of this effect were described in Ref. [5], where more than 1000 atoms were blockaded, and in Refs. [6,7], where the blockade effect was demonstrated between two individual atoms. Reference [8] provided spectroscopic evidence for the dipole-dipole interaction between cold Rydberg atoms. As a final example of basic phenomena, Ref. [9] gave experimental and theoretical evidence for spatially resolved observation of the effect of dipole-dipole interaction between Rydberg states.

In this paper, we don't address how the atoms could be placed in a lattice but note that there have been several investigations concerned with creation of a Rydberg gas on a lattice. Reference [10] has successfully trapped Rydberg atoms in an optical lattice, but this situation could also be created by taking ground-state atoms trapped in an optical lattice and exciting them to a Rydberg state. Reference [11] gave results of calculations that showed an optimal choice in the laser parameters could lead to the Rydberg atoms being in a regular spatial array, even though the ground-state atoms are randomly distributed in a gas. Again, by detuning the laser excitation of the Rydberg atoms, Ref. [12] gave experimental evidence for an antiblockade. Although they do not use Rydberg atoms as the element in the dipole-dipole interaction, Ref. [13] uses polar molecules confined in an optical lattice to investigate the time evolution of coherently excited dipoles.

Finally, the present work only treats the case of a single exciton moving through a lattice. There have been many studies of the many exciton case for Rydberg gases (e.g., see Refs. [14–19]), but the behavior of many excitons is beyond the scope of this paper.

*robichf@purdue.edu

This paper explores the role of randomness in the coherent motion of a Rydberg excitation of one type through a sea of Rydberg atoms. Although we only consider the case of a simple excitation, it is possible that more complicated cases (e.g., like the dressed atom case of Ref. [20]) would also be possible. We investigate the case of having the atoms placed on a lattice of sites with a specified amount of randomness either in the displacement of the atoms or the fraction of sites with missing atoms. Within investigations using Rydberg atoms, Refs. [21,22] have addressed randomness within a lattice of atoms, up to six sites in Ref. [21] and two sites in Ref. [22]. Also, Refs. [23,24] investigated how an exciton hops through a completely random Rydberg gas. Lastly, Refs. [25,26] treated the case of exciton motion with "heavy-tailed disorder" in the diagonal elements of the Hamiltonian.

In this paper, we have calculated the distribution of distances through which the excitation moved as a function of time for one-, two-, and three-dimensional lattices with varying amounts of disorder. We also investigate the unphysical $t \rightarrow \infty$ limit of the distribution of distances as a way to determine whether the motion was only slowed by the randomness or whether the excitation was localized.

The question of randomness in this system allows us to connect to Anderson localization [27,28], which has been observed in many systems including light traveling in a dielectric [29]. For short-range Hamiltonians, one-dimensional lattices have all eigenstates localized even for small amounts of disorder. We find that the motion of the excitation due to the dipole-dipole interaction also has every state localized. However, the distribution of distances has a stretched exponential decay for small to intermediate distances and a power-law decay for larger distances. For two and three dimensions, we find that almost no states are localized for weak randomness. Even for strong randomness, only a small fraction of states are localized. This result matches the finding of the authors of Ref. [30], who found an absence of Anderson localization of light moving through random point scatterers; the Hamiltonian for their case is similar to that in this paper except that the dipole-dipole interaction includes retardation effects. Finally, we note that the dipole-dipole interaction has the same form for magnetic and electric dipoles. Thus, although the details may differ, our results are also applicable to atoms with magnetic dipoles trapped in an optical lattice.

Atomic units are used unless explicit SI units are given.

II. COMPUTATIONAL METHOD

To obtain specific results, we solved for a particular case of dipole motion through a Rydberg gas. We treat the case where one atom is a p state and all of the other atoms are s states. The two states should have similar principle quantum number so that the dipole coupling between states is as large as possible. For the cases treated in this paper, we chose the $30s$ and $30p$ states of Rb.

A. Hamiltonian

This special case (p-state coherent motion through a sea of s states) is treated as Eq. (6) in Ref. [21]. The basis states can be labeled as $|i,m\rangle$ meaning the p state is at site i with angular momentum projection m. In this special case, the nonzero matrix elements reduce to

$$V_{im,i'm'} = -\sqrt{\frac{8\pi}{3}}\frac{\left(d_{n_a 1,n_b 0}\right)^2}{R^3} \times (-1)^{m'}\begin{pmatrix} 1 & 1 & 2 \\ m & -m' & m'-m \end{pmatrix} Y_{2,m'-m}(\hat{R}), \tag{1}$$

where the $d_{n_a 1,n_b 0}$ is the reduced matrix element between the p state with principle quantum number n_a and the s state with principle quantum number n_b, $(\ldots)$ is the usual $3j$ coefficient, and $\vec{R} = \vec{r}_i - \vec{r}_{i'}$ is the displacement vector between sites i and i'.

For the general case, the nonzero matrix elements are complex. In order to treat the largest number of atoms, we further restricted the p state to have $m = 0$. This can be accomplished experimentally by having an external field so that the $m = 0, 1, -1$ states are sufficiently separated in energy so that the motion does not mix m. Now the basis state can be designated solely by the site i and the nonzero matrix elements reduce to

$$H_{ii'} = V_{ii'} = -\frac{2}{3}P_2(\cos\theta_{ii'})\frac{\left(d_{n_a 1,n_b 0}\right)^2}{R^3}, \tag{2}$$

where $P_2(x) = (3x^2 - 1)/2$ is a Legendre polynomial and $\cos\theta_{ii'} = (z_i - z_{i'})/R$. This expression is only for $i \neq i'$; when $i = i'$, the matrix element is zero: $H_{ii} = 0$. By choosing $m = 0$ for the p state, the Hamiltonian will be real, symmetric which means the eigenvectors and eigenvalues will be real; this will reduce the amount of computer memory and time needed for the calculations. In all of the calculations, we use wrap boundary conditions in order to get better estimates of infinite size systems.

B. Randomness

We performed calculations for two kinds of randomness in the system.

Positional randomness has an atom at every site but there is a random shift of each atom. The x position of the ith atom is shifted from the perfect placement by an amount $(\chi - 0.5)\eta\delta x$, where χ is a random number with a flat distribution between 0 and 1 and δx is the spacing of atoms in the x direction. There is a similar randomness introduced into the y position for the two- and three-dimensional calculations. Finally, there is a similar randomness introduced in the z position for the three-dimensional calculation. The random shift for each direction is independent. Thus the randomness is only in the directions of the lattice position of the atom (in one dimension, the randomness is only in the x placement, etc.). The parameter η characterizes the amount of randomness. When $\eta = 0$, the system is a perfect lattice. We performed calculations for $\eta = 0$, 0.1, 0.2, 0.3, 0.4, and 0.5.

Filling randomness has the atoms placed perfectly on a lattice but each site may or may not be occupied. We did this calculation by generating a random number for each site. If the random number was greater than a parameter ζ, then the site would be occupied. On average, the number of occupied sites is $1 - \zeta$ times the number of sites in the lattice, and,

thus, ζ is the average fraction of missing sites. To compare with calculations of positional randomness, we compare cases where the lattice sizes are the same. We performed calculations for $\zeta = 0$, 0.1, 0.2, 0.3, 0.4, and 0.5.

C. Distribution of translation distances

We were interested both in the time dependence of how an excitation moves through an imperfect lattice and in the asymptotic, $t \to \infty$, distribution of sites the excitation can reach. If we were only interested in the time dependence of the motion, we could compute the distribution using several different methods for solving the time-dependent Schrodinger equation. However, the asymptotic distribution can be found simply from the eigenvalues and eigenvectors of the Hamiltonian; since we needed the eigenvalues and eigenvectors for the asymptotic calculation, we also used them for the time-dependent calculations.

The amplitude that an excitation starts at site i at $t = 0$ and coherently moves to site j at time t can be found from the eigenvalues and eigenvectors as

$$A_{j\leftarrow i}(t) = \sum_{\alpha} U_{j\alpha} e^{-iE_\alpha t} U^{\dagger}_{\alpha i}, \tag{3}$$

where the U and E_α are the eigenvectors and eigenvalues of the Hamiltonian described in the previous section,

$$\sum_{i} H_{ji} U_{i\alpha} = U_{j\alpha} E_\alpha. \tag{4}$$

The probability for the excitation to start at site i and move to site j at time t is simply

$$P_{j\leftarrow i}(t) = |A_{j\leftarrow i}(t)|^2, \tag{5}$$

which is the standard definition for probability.

The asymptotic probability to start at site i and be at site j can be defined as

$$P_{j\leftarrow i}(\infty) \equiv \lim_{t\to\infty} \frac{1}{T} \int_{t}^{t+T} P_{j\leftarrow i}(t')dt', \tag{6}$$

where $T \gg \hbar/\Delta E$ with ΔE the smallest energy difference in the system. One can show that this is equivalent to

$$P_{j\leftarrow i}(\infty) = \sum_{\alpha} |U_{i\alpha}|^2 |U_{j\alpha}|^2. \tag{7}$$

Once we have the probability for an excitation starting at a site i to be at a site j, the calculation of the distribution of translation distance can be obtained by binning. The probability to have moved to a site a distance between r and $r + \delta r$ is defined as $D(r)\delta r$. With this definition, the distribution of translation distances is given as

$$D(k\delta r,t) = \frac{1}{N\delta r} \sum_{i,j} P_{j\leftarrow i}(t) \Xi(r_{ij} - k\delta r), \tag{8}$$

where k is a non-negative integer, $r_{ij} = |\vec{r}_i - \vec{r}_j|$ is the distance between sites i and j, and $\Xi(x)$ equals 1 for $0 < x < \delta r$ and is zero otherwise. Of course, the algorithm we use to implement this definition involves taking the integer part of $r_{ij}/\delta r$ to find k. In our calculations, we average the distribution of translation distances over many different random configurations to obtain our final results.

For one dimension, the $D(r)$ will be a decreasing function of r because the excitation will tend to be near its original position. For higher dimension, the $D(r)$ can exhibit a more complicated dependence with r because there are more sites between r and $r + \delta r$ as r increases. In two dimensions, the number of sites between r and $r + \delta r$ increases linearly with r, while in three dimensions it increases quadratically.

III. RESULTS

In all of our calculations, we use the $30s$ and $30p$ states of Rb as our "sea" and "excitation" states, respectively. The size of these states is less than 0.1 μm. The standard step distance between atoms will be 10 μm. Thus the interactions higher order than dipole-dipole should be negligible. These states have dipole matrix element $d_{30s,30p} = 846$ a.u.; this value was obtained using the numerical method described in Ref. [31] but based on the updated quantum defects in Ref. [32]. For the one- and two-dimensional calculations, the atoms will be confined in the xy plane, which means there is no angular dependence to the matrix elements coupling different states. For the three-dimensional calculation, there is an angular dependence due to the $\cos^2(\theta_{ii'})$ term in the matrix element.

A useful quantity is the energy scale of the matrix element between nearest neighbors: $E_{sc} \sim d^2/R^3 = 1.06 \times 10^{-10}$ a.u. We can convert this to a time scale by $t_{sc} = 2\pi/E_{sc} = 5.93 \times 10^{10}$ a.u., which is 1.43 μs. This gives a sense of the time scale needed for the p-state character to move from site to site.

A. One dimension

In this section, we present the results of our calculations for a one-dimensional lattice. For the positional randomness, the atoms are only shifted in the x direction.

1. Positional randomness

Figure 1 gives an indication of how the p state moves away from the atom it starts on. This figure shows the distribution of translation distances, Eq. (8), times the lattice spacing, 10 μm. Thus the y axis is the probability to find the p state on a lattice site a distance r from its initial position. The distribution for times of 1, 2, 3, 4, and 5 μs are shown for different levels of positional randomness. We do not show the calculations for $\eta = 0$ (a perfect lattice) because it hardly differs from the $\eta = 0.1$ case.

There are some clear trends worth noting. For the $\eta = 0.1$ case, the p state is an increasingly greater distance from the initial position as time increases. Over this time scale, or equivalently this translation distance, the small randomness does not strongly affect the motion through the lattice. One interesting feature is the time scale for motion. Although the nearest-neighbor interaction energy gives a time scale of 1.43 μs, the p state has moved $\simeq$14 lattice spacings in 5 μs (approximately three scaled time units). Thus the motion is somewhat faster than might be expected from a crude estimate using the nearest-neighbor energy.

For larger randomness, the motion becomes increasingly restricted. Comparing the $\eta = 0.1$ and $\eta = 0.2$ cases, it appears that the farthest extent of the motion is approximately the same (about 14 sites), but the probability to be in the

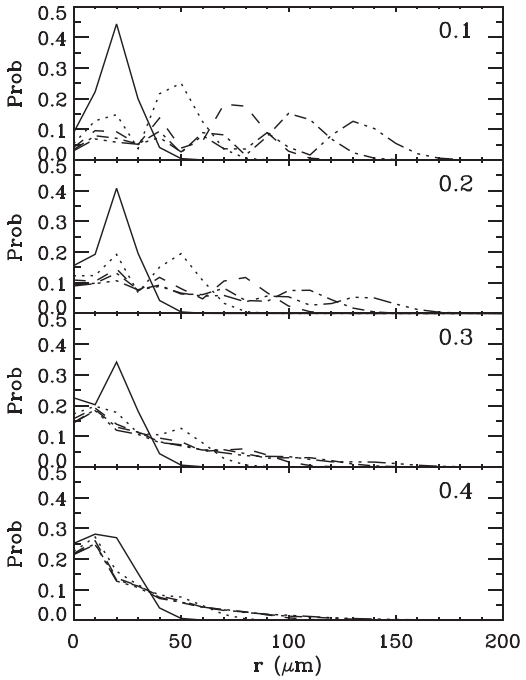

FIG. 1. Probability for the p state to be a distance r from its starting point averaged over a radial region equal to a lattice spacing. All of these calculations are for one dimension and have positional randomness with the top graph having $\eta = 0.1$ and the bottom graph having $\eta = 0.4$. The solid line is at a time of 1 μs, the dotted line is at 2 μs, the dashed line is at 3 μs, the dot-dash line is at 4 μs, and the dash-dot-dot-dot line is at 5 μs. Since the perfect lattice spacing is 10 μm, the graphs show the region within 20 lattice spacings.

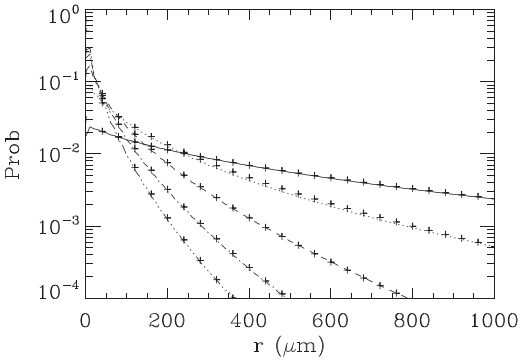

FIG. 2. Asymptotic in time probability for the p state to be a distance r from its starting point averaged over a distance region equal to a lattice spacing. All of these calculations are for one dimension and have positional randomness with solid line corresponding to $\eta = 0.1$, the dotted line to $\eta = 0.2$, the dashed line to $\eta = 0.3$, the dash-dot line to $\eta = 0.4$, and the dash-dot-dot-dot line corresponding to $\eta = 0.5$. These distributions are fit by the stretched exponential decay $\exp(-[r/r_c]^\alpha)$ with $\alpha = 0.57 \pm 0.02$ and r_c decreasing with increasing randomness. The $+$'s are the fits to the calculations with parameters given in the text.

furthest peak is $\sim 1/3$ as much for the larger randomness. For the $\eta = 0.3$ and 0.4 cases, it appears that the distribution hardly evolves for later times which indicates the p state is restricted to the region near where it started with the range decreasing with increasing η. The $\eta = 0.5$ distributions are similar to those shown for $\eta = 0.4$ but with the distance scale shrunk by approximately 20%.

An interesting question is whether the motion of the p state is actually restricted or whether its movement is only slowed down. To address this, we can use Fig. 2 to show that the range is restricted. This figure shows the asymptotic in time probabilities for different amounts of positional randomness [the asymptotic probability to move from site i to site j is given in Eq. (7)]. All of the distributions have two kinds of decays. The initial, fast decrease (to probabilities of $\sim 10^{-6}$) has the form of a stretched exponential. We fit these distributions using a simple function of the form $C \exp(-[r/r_c]^\alpha)$ down to the values of the probability of 10^{-10} or out to distances of 10^4 μm which is 1000 sites. We found that $\alpha = 0.57 \pm 0.02$ for all cases; the $+$'s in Fig. 2 show the fits to the data to give an idea of the accuracy. The "localization length scale," r_c, decreases with increasing randomness approximately as $1/\eta^2$, although this trend should be considered qualitative only because the "best" value for r_c depends on the choice of α. Our fit values for α, r_c are $(0.59, 210\ \mu\text{m})$ for $\eta = 0.1$, $(0.55, 45\ \mu\text{m})$ for $\eta = 0.2$, $(0.58, 22.8\ \mu\text{m})$ for $\eta = 0.3$, $(0.58, 12.3\ \mu\text{m})$ for $\eta = 0.4$, and $(0.58, 8.4\ \mu\text{m})$ for $\eta = 0.5$. The slow decay seems to be a power law although the power could not be accurately found by fitting because the data was noisy at these low probabilities. A decrease like $1/r^6$ or $1/r^7$ is consistent with the data. The fact that the data has a power-law decrease at large r is due to the long-range nature of the interaction between the different basis functions.

For the $\eta = 0.1$ case, we performed a calculation with 16 000 sites. If there is one extended state, then the smallest probability for the asymptotic distribution would be $\sim 2/16\,000^2 \sim 8 \times 10^{-9}$. In our calculation, the smallest probability was $\sim 10^{-12}$. This means there are *no* extended states for this level of randomness; thus *all* states have a restricted range as would be expected for Anderson localization.

2. *Filling randomness*

Figure 3 shows how the p state moves away from its initial position for different fractions of randomly missing atoms. As with Fig. 1, the plots show the distribution of translation distances, Eq. (8), times the lattice spacing, 10 μm, at different times; the different lines correspond to different durations (1, 2, 3, 4, and 5 μs).

There is a similar behavior to that in Fig. 1. The case of least randomness has the maximum extent of the motion (approximately 14 sites) nearly the same as the case of no randomness. However, there is less probability to reach the furthest extent. As with Fig. 1, the motion becomes increasingly restricted with increasing randomness. Also, the p state seems to have reached the limit of its range by ~ 5 μs for the most random cases. Comparing the results from the two types of randomness and setting $\eta = \zeta$, it appears that missing sites have a larger effect on the motion. For example, having 1/10 of the atoms missing (i.e., $\zeta = 0.1$) has a larger effect than having all of the atoms randomly moved by a distance of $\delta x/10$ (i.e., $\eta = 0.1$).

As with Fig. 2, we can investigate whether the range is actually restricted by examining the asymptotic in time distribution. These results are shown in Fig. 4 and show a faster

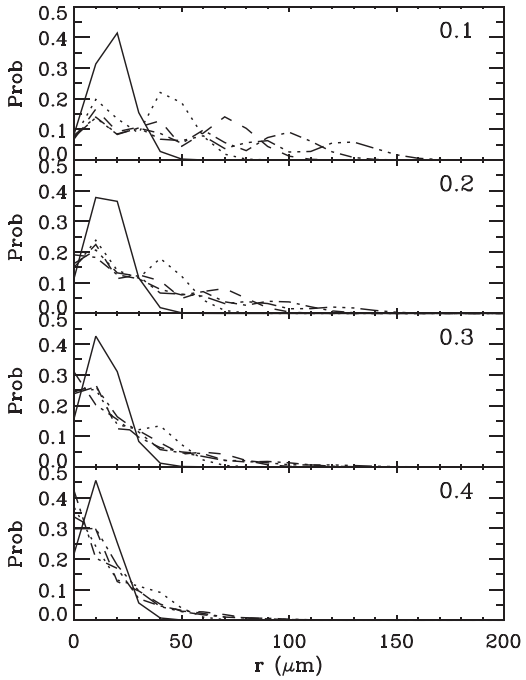

FIG. 3. Same as Fig. 1 but for filling randomness. The plots are for different vacancy fractions ζ.

decrease with distance compared to Fig. 2. The distribution becomes noisy for probabilities less than $\sim 10^{-7}$. As with Fig. 2, there is a fast decrease followed by a more slowly decreasing tail for probabilities less than $\sim 10^{-6}$. The more slowly decreasing part of the distribution was more prominent than for positional randomness so we were able to fit both the fast and slow decay parts of the distribution. We again found that the fast decay had the form of a stretched exponential while the slow decay had the form of high power. Because the slow decay was small there was a range of powers that seemed to work nearly as well but a $1/r^7$ seemed to do best. The form

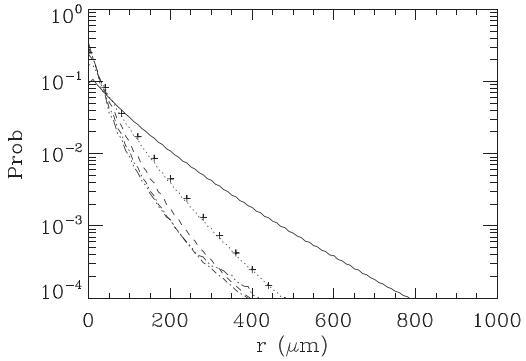

FIG. 4. Same as Fig. 2 but for filling randomness. The solid line corresponds to $\zeta = 0.1$, the dotted line to $\zeta = 0.2$, the dashed line to $\zeta = 0.3$, the dash-dot line to $\zeta = 0.4$, and the dash-dot-dot-dot line corresponds to $\zeta = 0.5$. These distributions are fit by the stretched exponential decay $\exp(-[r/r_c]^\alpha)$ plus a power law with $\alpha = 0.78 \pm 0.03$ and r_c decreasing with increasing randomness. The +'s are the fit to the $\eta = 2$ result: $0.26\ \exp[-(r/35\ \mu\text{m})^{0.80}] + 1.3 \times 10^{-4}[1.5\ \text{mm}/(r + 1.5\ \text{mm})]^7$.

we fit to was $C\ \exp(-[r/r_c]^\alpha) + B/(r + 1.5 \times 10^{-3}\ \text{m})^7$. We found that $\alpha = 0.78$ worked best for all cases with a spread of ± 0.03; the +'s in Fig. 2 show the fit for the $\eta = 0.2$ case to give an idea of the accuracy. Our fit values are 64 μm for $\zeta = 0.1$, 35 μm for $\zeta = 0.2$, 26 μm for $\zeta = 0.3$, 23 μm for $\zeta = 0.4$, and 21 μm for $\zeta = 0.5$.

Comparing Figs. 2 and 4, it's clear that the filling randomness leads to a smaller range if we take $\sim 10^{-4}$ as the condition. However, the localization lengths, which give the $1/e$ condition, can be smaller or larger depending on the amount of randomness. The reason for the difference in interpretation is the larger power in the stretched exponential for filling randomness.

For the $\zeta = 0.1$ case, we performed a calculation with 8000 sites. If there is one extended state, then the lowest probability for the asymptotic distribution would be $\sim 2/8000^2 \sim 3 \times 10^{-8}$. In our calculation, the smallest probability was $\sim 10^{-14}$. This means there are *no* extended states for this level of randomness; thus, as with the positional randomness, *all* states have a restricted range as would be expected for Anderson localization.

B. Two dimensions

In this section, we present the results of our calculations for a two-dimensional, square lattice. For the positional randomness, the atoms are only shifted in the x and y directions. The two-dimensional calculations are difficult to converge because the number of atoms increases quadratically with the linear lattice dimension. The time-dependent calculations shown in Fig. 5 are converged with respect to the number of lattice sites. None of the asymptotic distributions are converged with respect to lattice size: even the calculations with the most randomness have a large fraction of extended states that cover the whole lattice.

For the two-dimensional case, we only show the result for the positional randomness. While the randomness from missing sites gave different results compared to the randomness from shifting position, we did not find a qualitative difference worth reporting.

1. Positional randomness

Figure 5 shows the distribution of translation distances at different times for four levels of randomness. As in Figs. 1 and 3, the least random case, $\eta = 0.1$, is very similar to the no randomness case. The $\eta = 0.1$ and 0.2 cases qualitatively differ from the same cases in one dimension (Fig. 1). For Fig. 5, the peak in the distribution is at smaller r, but the 5 μs distribution noticeably differs from zero for a range more than twice that in Fig. 1. These differences are a reflection of the different band structure for two dimensions compared to one dimension (Figs. 2 and 3 of Ref. [21]). The $\eta = 0.3$ and 0.4 cases do not appear to be qualitatively different from the corresponding cases in Fig. 1. They both appear to have reached their maximum extent by approximately 5 μs. The $\eta = 0.3$ case has a larger extent than the 0.4 case, which is expected since larger randomness should more strongly confine the p excitation.

As with Figs. 2 and 4, we can investigate whether the motion is slowed by the disorder or is stopped by plotting

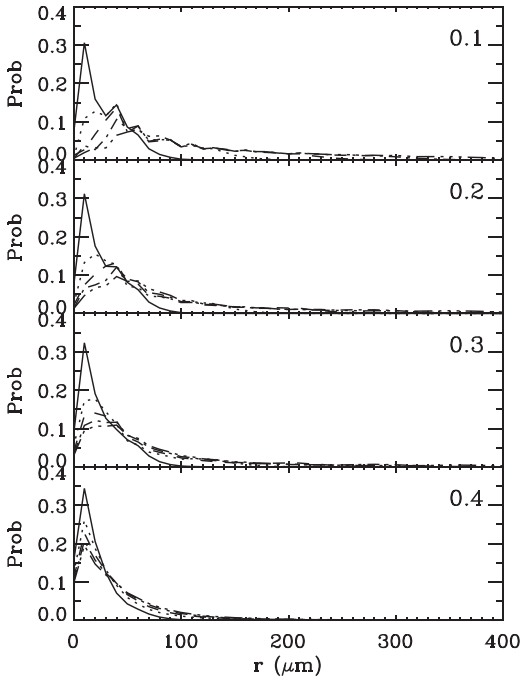

FIG. 5. Same as Fig. 1 but for a two-dimensional lattice. The results are for a 200×200 lattice; thus all of these results are converged. Note the different shape of the distribution and the farther extent compared to Fig. 1, which is the result of the p state having more atoms to interact with.

the asymptotic in time distribution of translation distances. Figure 6 shows this for the five different levels of positional randomness for a lattice of 200×200 atoms. Notice that Fig. 6 has a linear y axis, whereas Figs. 2 and 4 have a log scale. Unlike the one-dimensional cases in Figs. 2 and 4, the probability extends to the edge of the lattice for all cases. Thus none of these curves are fully converged. The case with the least randomness, $\eta = 0.1$, is nearly indistinguishable from the no randomness calculation; the probability increases linearly with distance because the number of sites between r and $r + 10\ \mu$m increases linearly with distance. This means

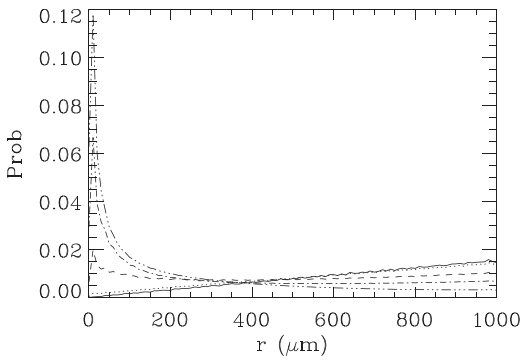

FIG. 6. Same as Fig. 1 but for a two-dimensional lattice. The results are for a 200×200 lattice. Since the wrap condition starts at 1000 μm and *all* cases have probability out to that distance, *none* of the calculations are converged. The linear increase with r for small η is due to the linear increase in the number of lattice sites with r. The peak at small r for larger η is from a fraction of localized states.

nearly all states for $\eta = 0.1$ extend for linear distance of over 100 lattice sites (i.e., nearly all states cover $\sim 10^4$ or more sites). Compare this with the $\eta = 0.1$ line in Fig. 2, which has an order of magnitude decrease in probability over the same range. The $\eta = 0.2$ case only slightly differs from the $\eta = 0.0$ case with slightly higher probability at smaller r and slightly lower probability at larger r; in Fig. 2, the $\eta = 0.2$ case had a decrease in probability of more than a factor of 100 over the range shown.

The cases with large randomness show a peak at small r which reflects the existence of localized states. Since the localized states do not extend to the edge of the lattice, the small r behavior is nearly converged for $\eta \geqslant 0.3$. Roughly, the region of convergence is $\leqslant 50\ \mu$m for $\eta = 0.3$ and $\leqslant 400\ \mu$m for $\eta = 0.5$. As with the smaller randomness cases, the localization region is much larger than that for the corresponding one-dimensional cases.

A final difference between the one- and two-dimensional calculation is how the results change with increasing randomness. The one-dimensional case had a smooth change in the asymptotic properties with increasing randomness. The two-dimensional case has almost no localized states for $\eta = 0.1$ and 0.2 with a big jump in number of localized states when going from $\eta = 0.2$ to 0.3.

C. Three dimensions

In this section, we present the results of our calculations for a three-dimensional, cubic lattice. The three-dimensional calculations are the most difficult to converge because the

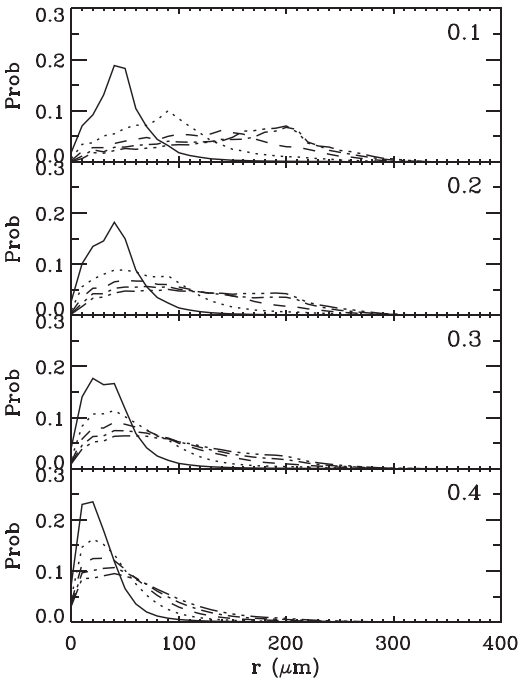

FIG. 7. Same as Fig. 1 but for a three-dimensional lattice. The results are for a $40 \times 40 \times 40$ lattice. Since the wrap condition starts at 200 μm, any of the probability distributions that extend past this are not converged. Note the different shape of the distribution and the farther extent compared to Figs. 1 and 5, which is the result of the p state having more atoms to interact with.

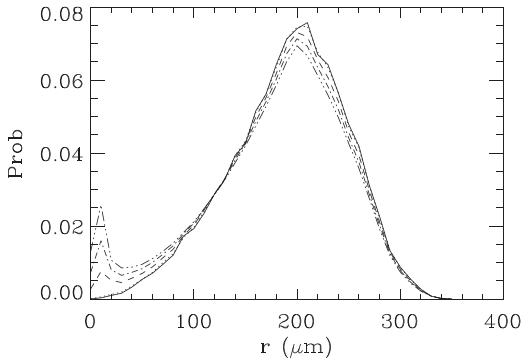

FIG. 8. Same as Fig. 1 but for a three-dimensional lattice. The results are for a $40 \times 40 \times 40$ lattice. Since the wrap condition starts at 200 μm and *all* cases have probability out to that distance, *none* of the calculations are converged. The quadratic increase with r is due to the quadratic increase in number of lattice sites with r out to 200 μm; the decrease for $r > 200$ μm is because the sphere extends outside of the cube in our calculation. The peak at small r for larger η is from a fraction of localized states.

number of atoms increase cubically with the linear lattice dimension. The largest calculation we performed was for a lattice of $40 \times 40 \times 40$ atoms (i.e., 64 000 total). The wrap boundary condition starts for atoms differing by 20 lattice sites in any direction. This means only the distances less than 200 μm do not depend on the wrap condition. The time-dependent calculations shown in Fig. 7 are not converged with respect to the number of lattice sites; the most nearly converged is the $\eta = 0.5$ case since, for that case, there was only a small probability to move more than 20 sites during the time shown. None of the asymptotic distributions are converged with respect to lattice size: even the calculations with the most randomness mostly consist of extended states that cover the whole lattice.

As with the two-dimensional case, we only show the positional randomness because the results of randomly removing atoms from sites are similar in character.

1. Positional randomness

Figure 7 shows the time dependence of the distribution of translation distance for four different levels of randomness. For the later times, only the $\eta = 0.4$ case is converged. The other calculations show a distinct change in slope at $r = 200$ μm. This is the distance corresponding to the wrap boundary condition and is an artifact. Despite the lack of convergence, there is some useful information that can be extracted. For example, it is clear that the p excitation moves even further than the two-dimensional case, Fig. 5. Thus the extra interactions that arise in higher dimension increase the speed of the motion. Another example is the relatively small effect that the randomness has. The $\eta = 0.1$ and $\eta = 0.2$ translation distributions are quite similar. Also, the $\eta = 0.4$ case still has a clearly evolving translation distribution at 5 μs, unlike the one- and two-dimensional cases.

Figure 8 gives the asymptotic distribution of translation distances for different η. The $\eta = 0.1$ and 0.2 cases hardly differ from the no randomness case. These distributions simply reflect the number of sites versus distance. For $r \leqslant 200$ μm, the number of sites between r and $r + \delta x$ increases quadratically with r. For larger r the number of sites decreases because the wrap cube is only filled out to 200 μm. For $r \geqslant 400$ μm there are no sites. The $\eta = 0.3$, 0.4, and 0.5 cases have a small peak at $r = 10$ μm, which arises from a small fraction of localized states. If one counts the extra probability for $r \leqslant 60$ μm, there is less than 10% of the states localized even for $\eta = 0.5$. Thus we expect that almost all excitations will be delocalized in three dimensions unless the randomness is even greater than the cases we considered.

IV. CONCLUSIONS

We have performed calculations for how a p state moves through a sea of s states due to the dipole-dipole interaction. We focused on how the motion changes when the atoms are positioned on a perfect lattice or have randomness. We considered two kinds of randomness: (1) the atoms have a slight, random shift from a position and (2) random atoms are removed from a perfect lattice. The case of a one-dimensional lattice gave the largest qualitative difference between the two kinds of randomness.

Our one-dimensional calculations with randomness resulted in all of the states being localized independent of the type of randomness or the size of randomness. The distribution of translation distances could be fit with a stretched exponential whose exponent depended on the type of randomness but did not depend on the size of the randomness. This suggests that even miniscule randomness would lead to all states being localized. It is not surprising that the one-dimensional cases with randomness lead to localization even for small amounts of randomness. However, the long-range interaction in the Hamiltonian leads to a power-law decrease with translation distance.

For two and three dimensions, it appears that the randomness slows down the motion but leads to localized states only for large randomness. It appears that the number of localized states goes to zero as the randomness decreases; the number of localized states might be zero even for small, but nonzero, randomness.

ACKNOWLEDGMENTS

This work was supported by the National Science Foundation.

[1] W. R. Anderson, J. R. Veale, and T. F. Gallagher, Phys. Rev. Lett. **80**, 249 (1998).

[2] I. Mourachko, D. Comparat, F. de Tomasi, A. Fioretti, P. Nosbaum, V. M. Akulin, and P. Pillet, Phys. Rev. Lett. **80**, 253 (1998).

[3] D. Jaksch, J. I. Cirac, P. Zoller, S. L. Rolston, R. Côté, and M. D. Lukin, Phys. Rev. Lett. **85**, 2208 (2000).

[4] D. Tong, S. M. Farooqi, J. Stanojevic, S. Krishnan, Y. P. Zhang, R. Côté, E. E. Eyler, and P. L. Gould, Phys. Rev. Lett. **93**, 063001 (2004).

[5] R. Heidemann, U. Raitzsch, V. Bendkowsky, B. Butscher, R. Löw, L. Santos, and T. Pfau, Phys. Rev. Lett. **99**, 163601 (2007).
[6] E. Urban, T. A. Johnson, T. Henage, L. Isenhower, D. D. Yavuz, T. G. Walker, and M. Saffman, Nat. Phys. **5**, 110 (2009).
[7] A. Gaëtan, Y. Miroshnychenko, T. Wilk, A. Chotia, M. Viteau, D. Comparat, P. Pillet, A. Browaeys, and P. Grangier, Nat. Phys. **5**, 115 (2009).
[8] K. Afrousheh, P. Bohlouli-Zanjani, D. Vagale, A. Mugford, M. Fedorov, and J. D. D. Martin, Phys. Rev. Lett. **93**, 233001 (2004).
[9] C. S. E. van Ditzhuijzen, A. F. Koenderink, J. V. Hernández, F. Robicheaux, L. D. Noordam, and H. B. van Linden van den Heuvell, Phys. Rev. Lett. **100**, 243201 (2008).
[10] S. E. Anderson, K. C. Younge, and G. Raithel, Phys. Rev. Lett. **107**, 263001 (2011).
[11] T. Pohl, E. Demler, and M. D. Lukin, Phys. Rev. Lett. **104**, 043002 (2010).
[12] T. Amthor, C. Giese, C. S. Hofmann, and M. Weidemüller, Phys. Rev. Lett. **104**, 013001 (2010).
[13] B. Yan, S. A. Moses, B. Gadway, J. P. Covey, K. R. A. Hazzard, A. M. Rey, D. S. Jin, and J. Ye, Nature (London) **501**, 521 (2013).
[14] H. Weimer, R. Löw, T. Pfau, and H. P. Büchler, Phys. Rev. Lett. **101**, 250601 (2008).
[15] S. Ji, C. Ates, and I. Lesanovsky, Phys. Rev. Lett. **107**, 060406 (2011).
[16] J. Otterbach, M. Moos, D. Muth, and M. Fleischhauer, Phys. Rev. Lett. **111**, 113001 (2013).
[17] P. Schauss, M. Cheneau, M. Endres, T. Fukuhara, S. Hild, A. Omran, T. Pohl, C. Gross, S. Kuhr, and I. Bloch, Nature (London) **491**, 87 (2012).
[18] D. Petrosyan, Phys. Rev. A **88**, 043431 (2013).
[19] W. Zeller, M. Mayle, T. Bonato, G. Reinelt, and P. Schmelcher, Phys. Rev. A **85**, 063603 (2012).
[20] S. Wüster, C. Ates, A. Eisfeld, and J. M. Rost, New J. Phys. **13**, 073044 (2011).
[21] F. Robicheaux, J. V. Hernández, T. Topçu, and L. D. Noordam, Phys. Rev. A **70**, 042703 (2004).
[22] S. Möbius, M. Genkin, S. Wüster, A. Eisfeld, and J. M. Rost, Phys. Rev. A **88**, 012716 (2013).
[23] S. Westermann, T. Amthor, A. L. de Oliveira, J. Geiglmayr, M. Reetz-Lamour, and M. Weidemüller, Eur. Phys. J. D **40**, 37 (2006).
[24] B. Sun and F. Robicheaux, Phys. Rev. A **78**, 040701 (2008).
[25] A. Eisfeld, S. M. Vlaming, V. A. Malyshev, and J. Knoester, Phys. Rev. Lett. **105**, 137402 (2010).
[26] S. M. Vlaming, V. A. Malyshev, A. Eisfeld, and J. Knoester, J. Chem. Phys. **138**, 214316 (2013).
[27] P. W. Anderson, Phys. Rev. **109**, 1492 (1958).
[28] B. Kramer and A. MacKinnon, Rep. Prog. Phys. **56**, 1469 (1993).
[29] D. S. Wiersma, P. Bartolini, A. Lagendijk, and R. Righini, Nature (London) **390**, 671 (1997).
[30] S. E. Skipetrov and I. M. Sokolov, Phys. Rev. Lett. **112**, 023905 (2014).
[31] J. H. Hoogenraad and L. D. Noordam, Phys. Rev. A **57**, 4533 (1998).
[32] W. Li, I. Mourachko, M. W. Noel, and T. F. Gallagher, Phys. Rev. A **67**, 052502 (2003).